Supplemental information

Supplemental Figures

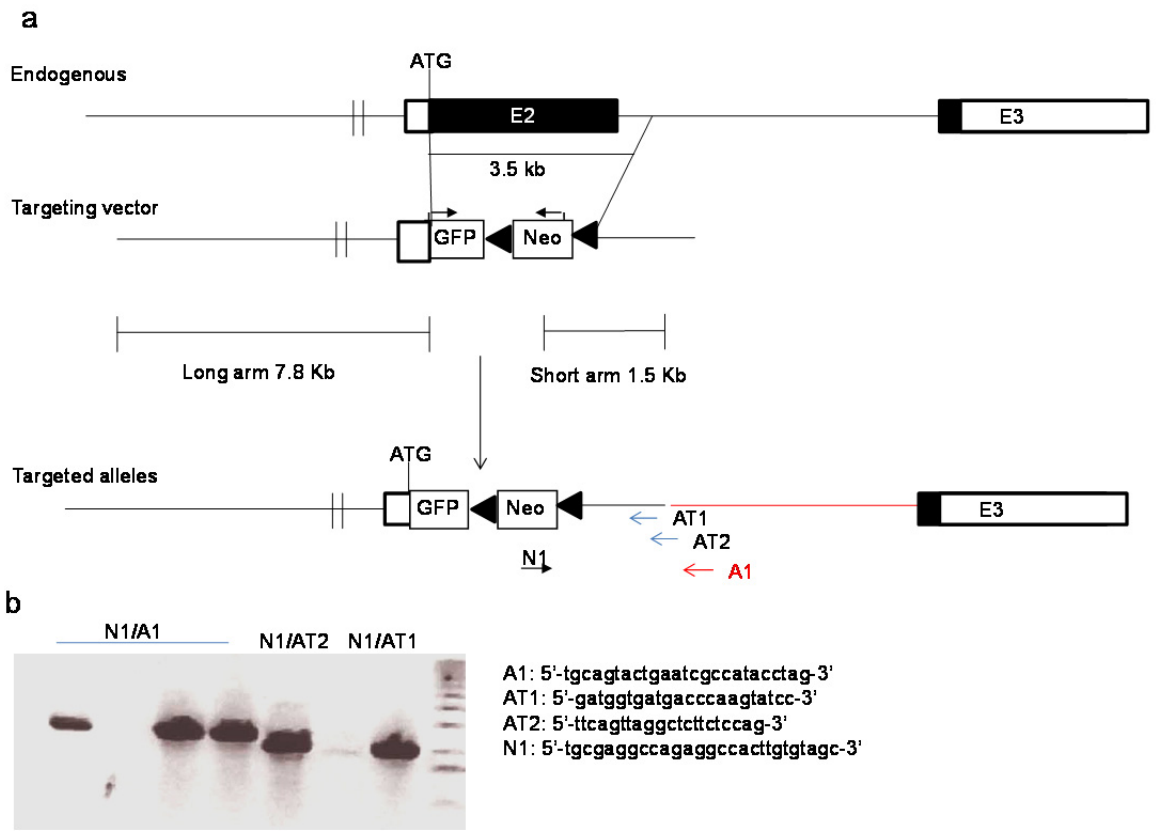

Fig. S1. Production of mice with targeted mutation of the *Fbxo30* gene. a. Diagram of gene targeting strategy and vectors used. The primers used for screening cells are also marked. b. PCR screening. Data show PCR results of 4 clones (3 positive and 1 negative) and positive controls. The primer sequences are shown on the right. PCR reactions using A1 with the N1 primer at the 5' end of the Neo cassette amplify 2.2 kb fragments. The control PCR reaction was done using AT1 and AT2, which is at the 5'

end of the SA inside the region used to create the targeting construct. These primers amplify bands of 2.0 and 2.1 kb, respectively, related to Figure 1.

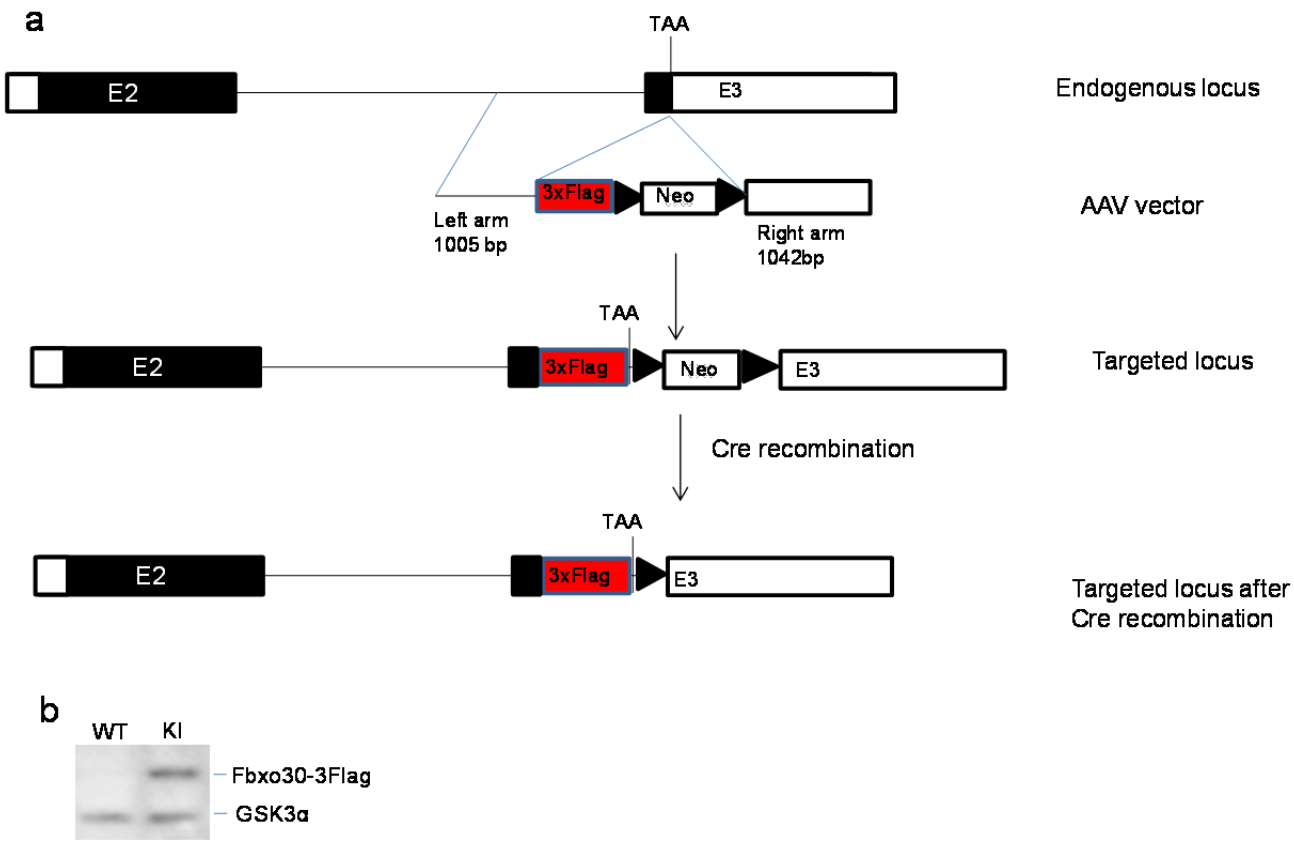

Fig. S2. Generation of HCT116 cell line with Flag-tagged endogenous *Fbxo30* gene. a. Diagram of constructs and knock-in strategy used. The upper panel shows the configuration of the *Fbxo30* gene and that of adeno-associated virus vector consisting of left homologous arm with sequencing encoding 3x flag epitope and right homologous arms. The middle panel shows the configuration of knock-in locus, with the Neo cassette. The lower panel shows the recombined locus with Cre-mediated deletion of the Neo cassette. The sequence of the recombinant locus as well as the vectors were confirmed by sequencing. b. Western blot confirmation of the *de novo* generation of the

fusion protein in the knock-in cells but not in the parental HT116 cell line. GSK3α was used as a loading control. Related to Figure 5.

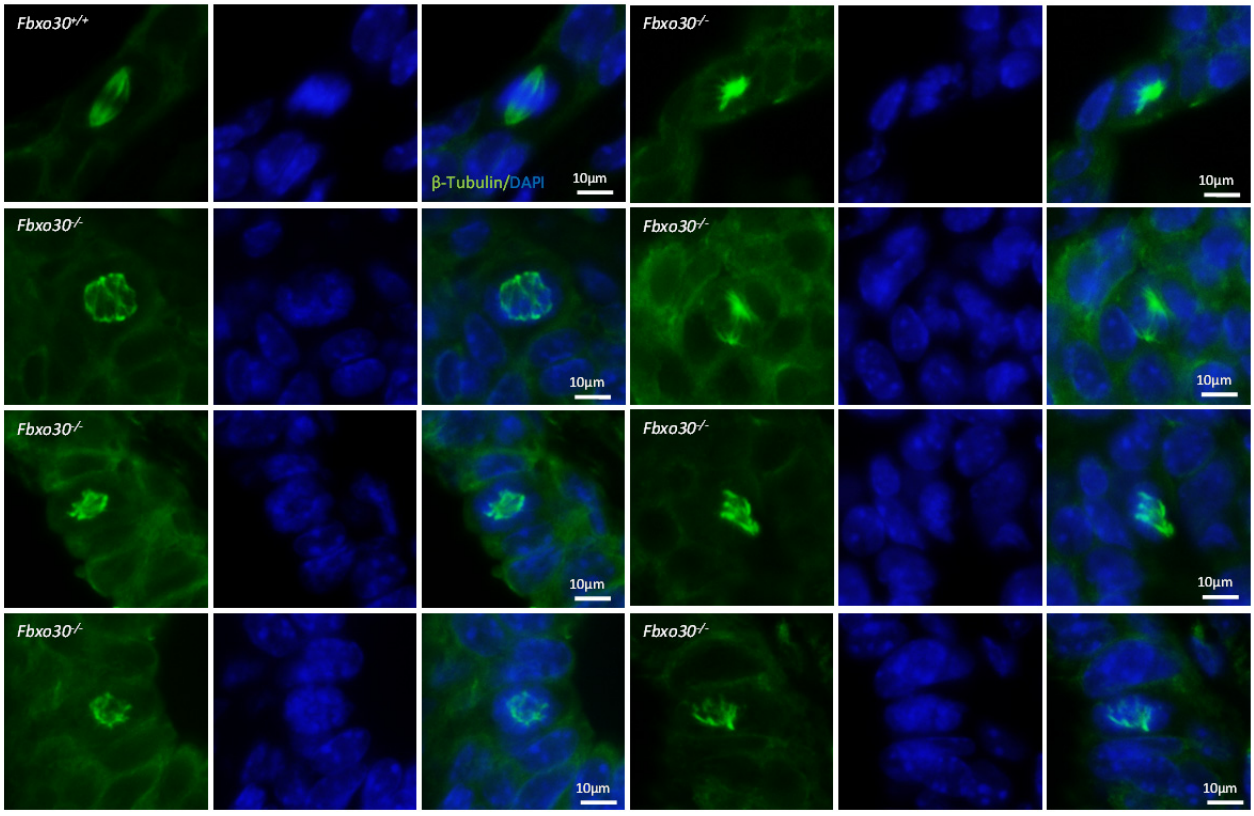

Fig. S3. Images of mitotic spindles in WT and *Fbxo30*$^{-/-}$ mammary glands. Paraffin sections of mammary glands from 8 or 24 weeks old mice (5 per group) were stained with anti-β-tubulin antibodies and DAPI. Only one mitotic spindle was found in all WT tissue examined, while more than 50 mitotic spindles were found in the same number of *Fbxo30*$^{-/-}$ mammary glands. Data shown include the WT mitotic spindle and 7 representative spindles in the *Fbxo30*$^{-/-}$ mammary glands. Parts of three images in the upper left panels were included in Fig. 4g. All mitotic spindle in the Fbxo30$^{-/-}$ glands are

abnormal based on the number and position of the spindles and the configuration of the chromatin. Related to Fig. 4.

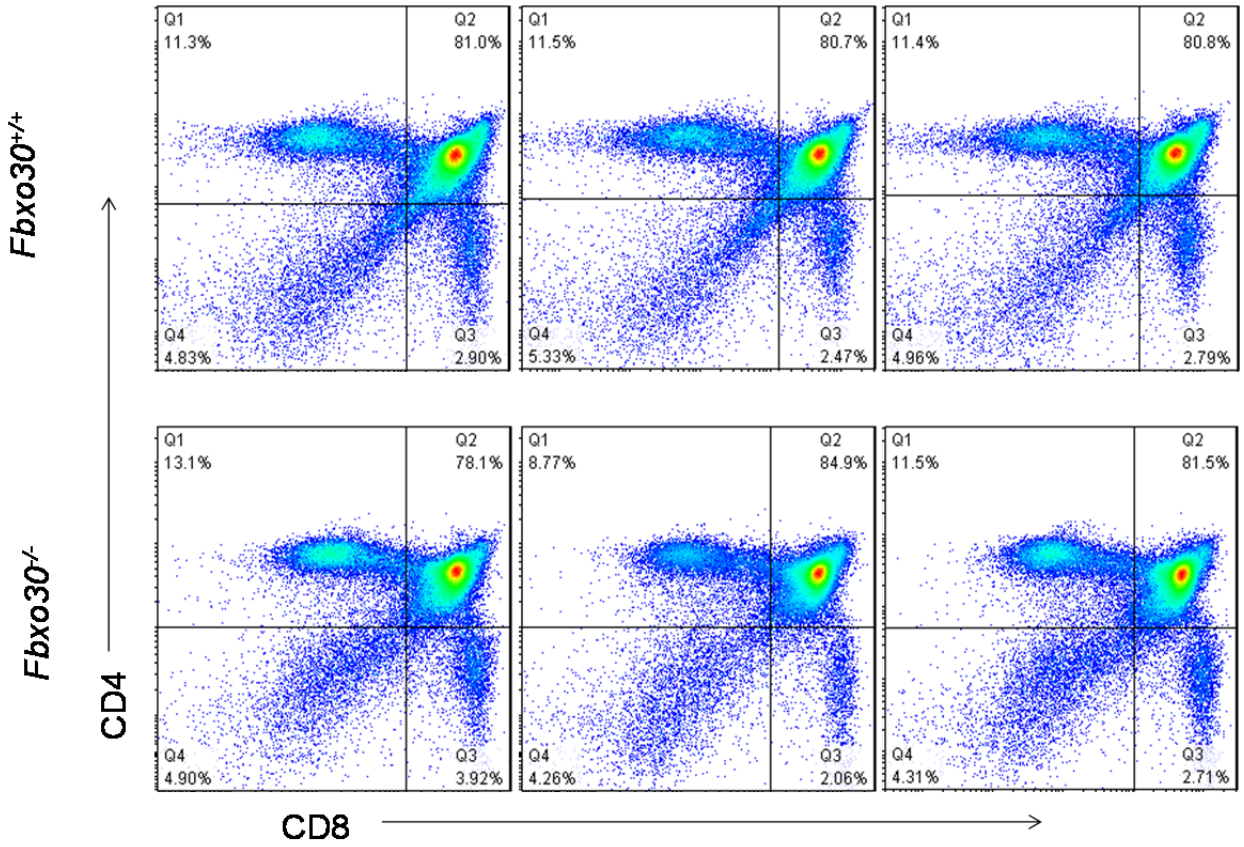

Fig. S4. Normal thymocyte development in *Fbxo30*$^{-/-}$ mice based on distribution of CD4 and CD8 markers. Three individual mice in each group were analyzed by flow cytometry. This experiment has been reproduced at least three times. Related to Figure 1.

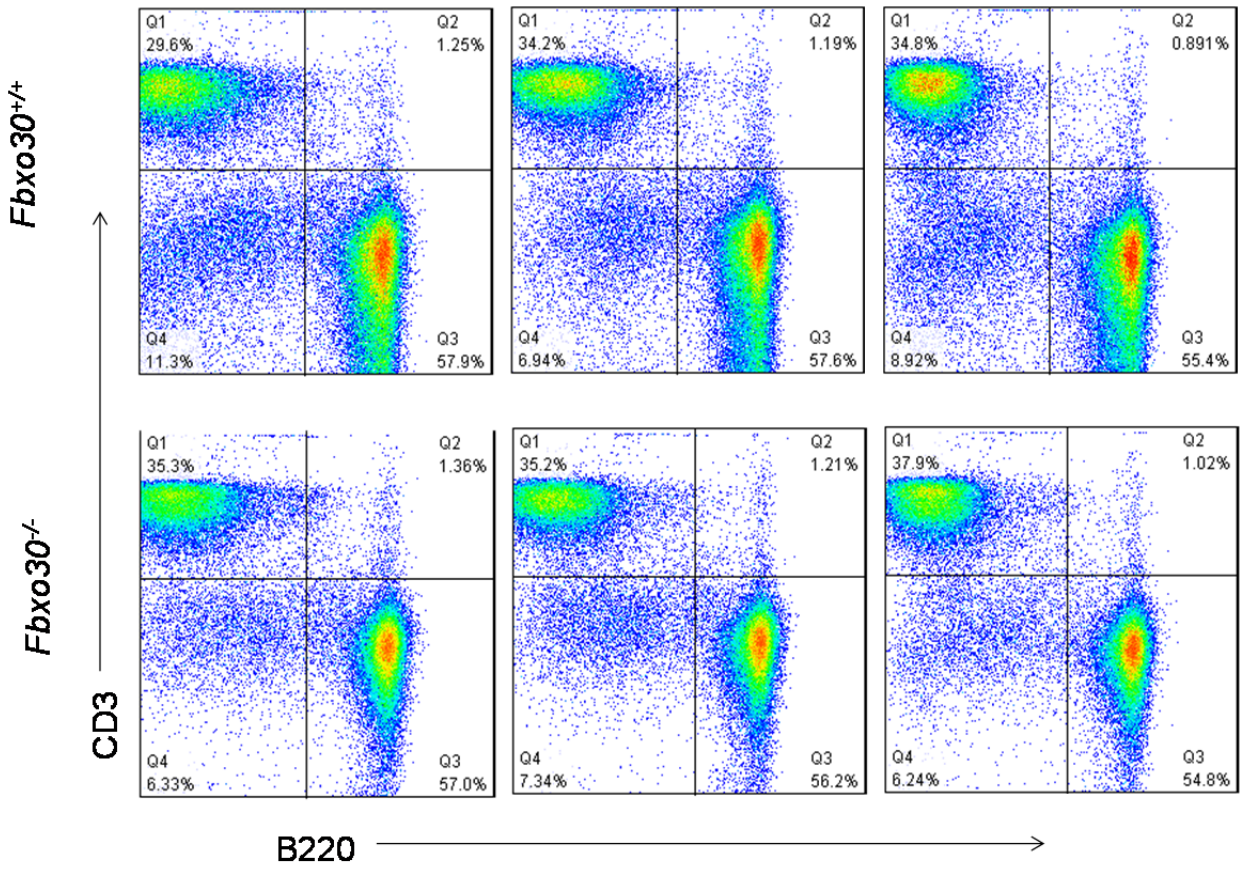

Fig. S5. Normal T and B cell compositions in *Fbxo30*$^{-/-}$ mice based on distribution of CD3 and B220 markers. Three individual mice in each group were analyzed by flow cytometry. This experiment has been reproduced at least three times. Related to Figure 1.

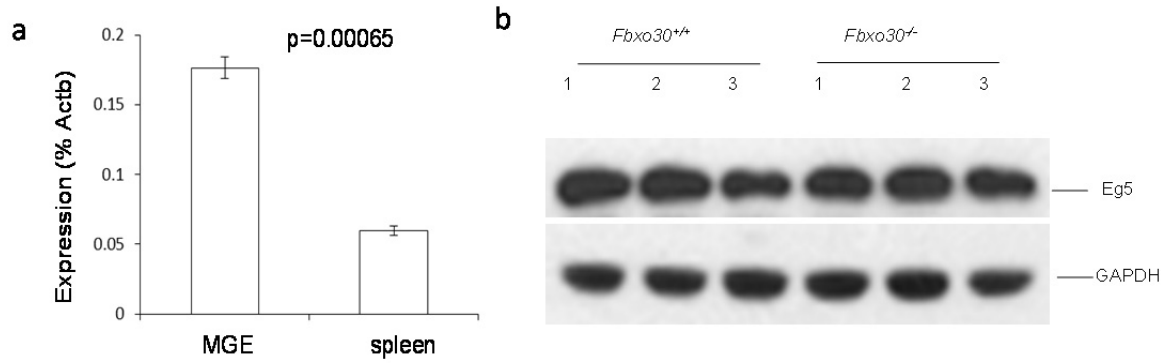

Fig. S6. a. Spleen cells express lower levels of *Fbxo30* mRNA than the mammary gland cells. The amounts of *Kif11* mRNA in freshly isolated MGE and spleen cells were measured by Q-PCR and expressed as % of mRNA from *Actb*, the gene that encodes β-actin. N=3. These data have been reproduced twice. b. Effect of *Fbxo30* mutation on Eg5 levels in spleen cells. The left panels are Western blots, showing the levels of EG5 in WT (+/+) and mutant (-/-) cells isolated from the spleen. Three different lanes per group represent samples from three different mice. The right panel shows quantitation after normalization against β-actin levels. Related to Figure 1.

Table S1. Maternal mutation of *Fbxo30* affects offspring survival of but not maternal fertility

Breeder		born	Postnatal death (1-3ds)	survival		% survival	Litters observed
female	male			female	male		
(-/-)	(-/-)	263	232	15	16	11.8	40
(-/-)	(+/-)	15	15	0	0	0	2
(-/-)	(+/+)	38	35	0	3	7.89	6
(+/-)	(-/-)	310	91	108	107	69.4	43
(+/-)	(+/-)	49	22	15	12	55.1	6
(+/-)	(+/+)	28	10	9	9	64.2	5
(+/+)	(-/-)	38	6	17	15	84.2	4
(+/+)	(+/-)	82	16	36	31	81.7	8
(+/+)	(+/+)	61	10	25	26	83.6	8

Related to Figure 1.